

1        **A New Application of Scanning Electrochemical Microscopy for the**  
2                    **Label-free Interrogation of Antibody-Antigen Interactions.**

3

4                    **Joanne L. Holmes<sup>1</sup>, Frank Davis<sup>1</sup>, Stuart D. Collyer<sup>1</sup>, Séamus P.J. Higson<sup>1\*</sup>**

5        *<sup>1</sup>Cranfield Health, Cranfield University, Cranfield, MK43 0AL, U.K.*

6        \*Correspondence should be addressed to s.p.j.higson@cranfield.ac.uk.

7

8        **Abstract**

9

10        Within this work we present a ‘proof of principle’ study for the use of scanning  
11        electrochemical microscopy (SECM) to detect and image biomolecular interactions in a  
12        label-free assay as a potential alternative to current fluorescence techniques.  
13        Screen-printed carbon electrodes were used as the substrate for the deposition of a dotted  
14        array, where the dots consist of biotinylated polyethyleneimine. These were then further  
15        derivatised, first with neutravidin and then with a biotinylated antibody to the protein  
16        neuron specific enolase (NSE). SECM using a ferrocene carboxylic acid mediator  
17        showed clear differences between the array and the surrounding unmodified carbon.  
18        Imaging of the arrays before and following exposure to various concentrations of the  
19        antigen showed clear evidence for specific binding of the NSE antigen to the antibody  
20        derivatised dots. Non-specific binding was quantified. Control experiments with other  
21        proteins showed only non-specific binding across the whole of the substrate, thereby  
22        confirming that specific binding does occur between the antibody and antigen at the

23 surface of the dots. Binding of the antigen was accompanied by a measured increase in  
24 current response, which may be explained in terms of protein electrostatic interaction and  
25 hydrophobic interactions to the mediator, thereby increasing the localised mediator flux.  
26 A calibration curve was obtained between  $500 \text{ fg mL}^{-1}$  to  $200 \text{ pg mL}^{-1}$  NSE which  
27 demonstrated a logarithmic relationship between the current change upon binding and  
28 antigen concentration without the need for any labeling of the substrate.

29

30 **Keywords:** Scanning Electrochemical Microscopy, Neuron Specific Enolase, Label-Free,  
31 Antibody

32

### 33 **1. Introduction**

34

35 In recent years there has been an increasing demand for the development of parallel  
36 analytical testing platforms and this has led to increased research into miniaturised  
37 biosensors, biosensor arrays, and chip based testing systems. Within the commercial  
38 market it is already possible to obtain DNA-based testing systems, however there is still  
39 an unmet need when considering the use of proteins as the functional units. This is  
40 possibly due in part to proteins being less stable and also their characteristic to denature  
41 once in contact with the surface to which they are immobilized.

42

43 The incorporation of antibodies into conducting polymer films was first reported in 1991  
44 [1]. Anti-human serum albumin (anti-HSA) was incorporated into a (poly)pyrrole film,  
45 which was galvanostatically polymerized onto a platinum wire substrate. When the

46 pyrrole anti-HSA was exposed to  $50 \mu\text{g mL}^{-1}$  HSA for 10 min, a new reduction peak was  
47 observed at a potential of +600 mV versus Ag/AgCl. Since this preliminary work there  
48 has been an increase in the development of electrochemical immunosensors, as reviewed  
49 previously elsewhere [2-4].

50

51 Previous work within our group has shown that up to 2-3  $\mu\text{g}$  of antibodies for bovine  
52 serum albumin (BSA) and digoxin may be successfully incorporated into conducting  
53 polymer films by entrapment in an electrochemically grown (poly)pyrrole film with no  
54 detrimental effect to antibody activity [5]. Further work utilized an ac impedance protocol  
55 as the method for interrogation for these films [6]. A protocol was then developed for  
56 immobilizing antibodies onto polyaniline-coated screen printed carbon electrodes which  
57 utilized the classical avidin-biotin interaction. This enabled the construction of  
58 immunosensors for the antibiotic ciprofloxacin [7, 8], the heart drug digoxin [9] and for  
59 myelin basic protein [10] - which could detect their respective targets with detection  
60 limits of  $1 \text{ ng mL}^{-1}$  of the target species. Later work utilized polyaniline microarrays as a  
61 substrate for the assembly of immunosensors for prostate specific antigen (PSA) [11] and  
62 the stroke marker proteins neuron specific enolase (NSE) [12] and S100[ $\beta$ ] [13], with  
63 greatly lowered limits of detection down to the level of  $1 \text{ pg mL}^{-1}$  of the target.

64

65 Biotin/avidin chemistry has been used extensively to modify electrode surfaces by protein  
66 immobilization. The attachment of a biotin molecule allows the immobilization of any  
67 biomolecule of the avidin family. Neutravidin protein is a deglycosylated version of  
68 avidin with four identical binding sites. It has a near neutral isoelectric point (IEP) which

69 minimizes non-specific interaction and like avidin itself has a strong affinity with biotin  
70 ( $K_D = 10^{-15} \text{ M}^{-1}$ ) [14,15]. Due to this strong interaction, the complex formation is nearly  
71 unaffected by extremes of pH or temperature, organic solvents, and denaturing agents.  
72 The tetravalent binding of neutravidin to biotin allows the construction of a molecular  
73 sandwich effect where the bound neutravidin is free to couple to a biotinylated antibody  
74 with the appropriate characteristics needed for the construction of a biosensor.

75

76 Enolase is a 78 kDa homo- or heterodimeric cytosolic protein produced from  $[\alpha]$ ,  $[\beta]$ , and  
77  $[\gamma]$  subunits. The  $[\gamma][\gamma]$  enolase isoform is most specific for neurons, and is referred to as  
78 NSE. Elevations of NSE in serum can be attributed to cerebral injury due to physical  
79 damage or ischemia caused by infarction or cerebral haemorrhage, coupled with  
80 increased permeability of the blood brain barrier. The serum concentration of NSE has  
81 also been reported to correlate with the extent of damage (infarct volume) and  
82 neurological outcome [16]. Additionally, a secondary elevation of serum NSE  
83 concentration may be an indicator of delayed neuronal injury resulting from cerebral  
84 vasospasm [17]. NSE, which has a biological half-life of 48 hours and is normally  
85 detected in serum at an upper limit of  $12.5 \text{ ng mL}^{-1}$  (160 pM), is typically elevated after  
86 stroke and cerebral injury. Serum NSE is elevated after 4 hours from onset, with  
87 concentrations reaching a maximum between 1-3 days after onset [18]. After the serum  
88 concentration reaches its maximum (maybe  $>300 \text{ ng mL}^{-1}$ , 3.9 nM), it gradually  
89 decreases to normal concentrations over approximately one week.

90

91 Scanning electrochemical microscopy (SECM) is a surface scanning probe technique that  
92 allows for the collection of high resolution electrochemical data on a variety of surfaces  
93 and has previously been used successfully to investigate various biological systems  
94 including cells [19-23], enzymes [24-27], and DNA [28-30].

95

96 We have, within this work, attempted to utilize the SECM to detect the binding of  
97 antibody layers to electrodes and to determine if these systems can be used for the label-  
98 free detection of NSE. This work is intended as a 'proof of principle' study to show the  
99 feasibility of antigen adsorption and imaging rather than the fabrication of either a  
100 sensitive antigen sensor or the detailed examination of the polymer and biomolecular  
101 films absorbed. Once a proof of principle has been demonstrated we will in future work  
102 move towards studying a range of antigens of various molecular sizes and investigate the  
103 possibility of fabricating one array containing a number of different antibodies of interest.

104

105

106

## 107 **2. Experimental Section**

108

### 109 **2.1 Chemicals and Reagents**

110

111 Ferrocene carboxylic acid, biotinylation kit (part no. BK101), neutravidin,  
112 polyethyleneimine (PEI) (MW = 50000) and BSA were purchased from Sigma-Aldrich  
113 (Gillingham, Dorset, UK). Disodium hydrogen orthophosphate monohydrate, sodium

114 dihydrogen orthophosphate 12-hydrate and sodium chloride (all 'AnalaR' grade) were  
115 purchased from BDH (Poole, Dorset, UK). All reagents were used without further  
116 purification. Commercial screen-printed carbon electrodes were obtained from  
117 Microarray Ltd. (Manchester, UK). NSE and monoclonal antibody against NSE - both  
118 with sodium azide preservative, and PSA were supplied by Canag Diagnostics, Ltd.  
119 (Gothenburg, Sweden).

120

121 For antibody and PEI biotinylation, the procedure outlined in the BK101 kit was followed  
122 (see manufacturer's instructions for details). Biotinylated antibodies were kept frozen in  
123 aliquots of 200  $\mu\text{l}$  at a concentration of 0.2  $\text{mg mL}^{-1}$  until required.

124 All water used was purified with an ELGA Purelab UHQ-II water system (Elga High  
125 Wycombe, UK). Phosphate buffer (PBS), pH 7.0 contained  $\text{NaH}_2\text{PO}_4$  (4  $\text{mmol mL}^{-1}$ ),  
126  $\text{Na}_2\text{HPO}_4$  (6  $\text{mmol mL}^{-1}$ ) and  $\text{NaCl}$  (132  $\text{mmol mL}^{-1}$ ).

127

128 SECM experiments were carried out using a Uniscan SECM270 (Uniscan Instruments  
129 Ltd, Buxton, UK). The SECM instrument (shown schematically in figure 1a) is composed  
130 of (1) an electrochemical cell, (2) a translational stage capable of high resolution  
131 movement in the X,Y and Z planes (sub-micron), (3) a bipotentiostat for the accurate  
132 control of the potential applied at the tip and/or substrate, (4) a hardware interface  
133 enabling the control of (1) and (2), and (5) a PC which provides an interface with the  
134 hardware – and allows the operator to accurately control the parameters of the SECM  
135 procedure. Pt counter electrodes and Ag/AgCl reference electrodes were also utilized as

136 shown in figure 1b. Ferrocene carboxylic acid ( $5 \text{ mmol l}^{-1}$  in pH 7.0 phosphate buffer)  
137 was used as the mediator (figure 1c).

138

## 139 **2.2 Substrate patterning**

140

141 In the immunosensors previously developed within our laboratory, cyclic voltammetry  
142 was utilized to deposit polyaniline films on the carbon electrodes [7-13]. This was  
143 deemed inappropriate for the preparation of electrodes to be interrogated by SECM as it  
144 is not possible to compare a modified region with an unmodified region. Any changes in  
145 the tip current obtained may be due to fluctuations in the background current and not due  
146 to changes in the charge transfer properties of the modified substrate. It was therefore  
147 decided that for SECM interrogation, the polyelectrolyte film should be patterned in an  
148 array dot format. By producing this pattern, background effects in the measured current  
149 could therefore be eliminated and any changes in the current over the modified surface  
150 would contrast with the current over regions of unmodified carbon. Since it would not be  
151 possible to use polyaniline in this format it was decided to use PEI which has previously  
152 been used within the group when interrogating DNA arrays with SECM [30].

153

154 A borosilicate glass capillary was pulled to an internal diameter of 80-100  $\mu\text{m}$  using a  
155 Narishige PP-830 pipette puller (Narishige International Limited, London, UK) and the  
156 tip polished to a flat finish. This capillary was then filled with a 1% biotinylated PEI  
157 solution and, using the micropositioning stage on the Uniscan SECM270, used to  
158 fabricate a biotinylated PEI array (figure 2). Each of the dots were distanced 300  $\mu\text{m}$

159 centre to centre and approximately 200  $\mu\text{m}$  in diameter. After patterning, the substrate  
160 was then rinsed with UHQ water. Once the area was dry 20  $\mu\text{l}$  of neutravidin (10 mg  
161  $\text{mL}^{-1}$  in water) were placed on the dotted microarray for 1 h, followed by rinsing with  
162 water. 20  $\mu\text{l}$  of biotinylated antibody (0.2 mg  $\text{mL}^{-1}$  in water, 1 h) were then added  
163 followed by further rinsing. Finally non-specific interactions were blocked by BSA ( $10^{-6}$   
164  $\text{mol L}^{-1}$  in PBS, 1 h).

165

### 166 **2.3 SECM studies**

167

168 A screen-printed carbon electrode substrate was placed in a plastic Petri dish and exposed  
169 to 5  $\text{mmol l}^{-1}$  mediator solution. The SECM working electrode tip and counter and  
170 reference electrodes were then immersed into the mediator solution. Prior to undertaking  
171 an area scan over the antibody/PEI functionalized regions, an approach curve experiment  
172 was conducted over the polycarbonate, non-conductive region of the substrate to estimate  
173 the tip-to-substrate distance (Tip Potential (E) = +0.45 V vs. Ag/AgCl; step size = 10  
174  $\mu\text{m}$ ). The tip was positioned at a distance at which the measured current was half that of  
175 the observed current with the tip a few mm distant from the surface of the screen printed  
176 electrode (effectively infinite on this scale) (approximately 70  $\mu\text{m}$  from substrate  
177 surface); this was to allow for the variation in topography and the height differential  
178 between this non-carbon region and the slightly raised carbon electrode surface - while  
179 also serving to reduce the risk of tip crash. After tip positioning, an area scan over the  
180 functionalised region was conducted with a step size of 10  $\mu\text{m}$ . At no point in the  
181 experiment was the substrate touched; this allowed any change in the observed tip current



182 to be attributed solely to changes in the charge transfer properties of the surface. In all  
183 cases the tip diameter was 8.5  $\mu\text{m}$ ; the scan rate used was 10  $\mu\text{m}$  per step throughout and  
184 there was no potential applied to the substrate.

185

186 After the first area scan experiment was conducted, the tip was retracted a known safe  
187 distance from the substrate. The mediator solution was then removed and the substrate  
188 gently rinsed with UHQ water before applying a solution containing complementary  
189 antigen over a range of concentrations or a non-complementary antigen. After exposure  
190 for 1 hour, the antigen solution was then removed and the substrate again rinsed before  
191 the re-introduction of fresh mediator solution. A second area scan experiment was then  
192 conducted over the same functionalised area as measured previously. The tip current data  
193 from the area scan before exposure was then subtracted from the tip current data  
194 following this exposure. Throughout all these experiments the sample substrate does not  
195 move at all, i.e. all exposures, rinsing steps etc are performed with the sample *in situ*. It is  
196 worth noting here that after each exposure and rinsing step the Petri dish is refilled with  
197 fresh mediator solution and the tip exactly repositioned, made possible using the XYZ  
198 micro-positioning stage of the SECM270. This allows precise and reproducible imaging  
199 of the same area of the electrode.

200

### 201 **3. Results and Discussion**

202

203 To ensure that changes occurring on the sensor surface were directly related to the  
204 hybridization of antibody and antigen, and not due to interference of mediator solution or

205 poor stability of the substrate, surface scans were undertaken of the antibody modified  
206 dotted arrays (figure 3a). The modified surface displays an array of peaks which  
207 correspond to decreases in the tip current. This can be accounted for by the  
208 polymer/antibody composite acting as a barrier to mediator diffusion to the surface,  
209 thereby diminishing the current since polyelectrolytes are known to act as barriers to ion  
210 migration [31].

211

212 After this initial scan, samples were incubated in purified water for 30 mins in parallel to  
213 the immunochemical exposures but in the absence of antigen. Following rinsing, fresh  
214 mediator solution was introduced. A scan of this surface is shown in figure 3b.

215 Subtraction of figure 3a from 3b (figure 3c) clearly shows only minimal variations,  
216 indicating that minimal changes in background current are seen and that there is no loss  
217 of material from the surface. Other techniques employed to dot down the array were  
218 investigated. These included the direct dotting of antibody onto the carbon surface,  
219 however, these proved to be unstable and deterioration of the array could be visualised as  
220 the scan progressed.

221

222 Binding experiments were performed by soaking the modified antibody dotted arrays in  
223 solutions of varying concentrations of the complementary antigen for 30 mins, followed  
224 by scanning in fresh mediator solution. A control was also run using  $5 \text{ pg mL}^{-1}$  PSA to  
225 ensure changes could be related to specific antigen/antibody binding rather than simple  
226 non-specific absorption of proteins to surfaces. Binding experiments were carried out  
227 using NSE solution with concentrations ranging from  $500 \text{ fg mL}^{-1}$  -  $200 \text{ pg mL}^{-1}$  in water.

228 Detailed results (figures 4a – c) are presented for the exposure to  $200 \text{ pg mL}^{-1}$ . Figure 4a  
229 depicts the scan over the dotted array before incubation, with figure 4b showing the scan  
230 taken after exposure to  $200 \text{ pg mL}^{-1}$  NSE. Figure 4c shows the difference between the  
231 two scans indicating changes to the tip current over both the carbon surface and the  
232 dotted substrate. Figure 4c shows that across the whole of the array there is a general  
233 increase in measured tip current. The change in tip current is, however, seen to be much  
234 greater in the areas of the PEI/biotinylated antibody dots than for the untreated carbon  
235 surface.

236

237 NSE is known to have both positively and negatively charged areas on the surface of the  
238 protein [32]. The cationic areas of the protein are capable of electrostatically attracting  
239 the ferrocene carboxylic acid (which is anionic at pH 7 due to ionisation of the acid  
240 group), thereby increasing the flux of the mediator to the microelectrode tip. There is also  
241 the possibility of hydrophobic interactions between the ferrocene unit and any  
242 hydrophobic regions of the NSE protein. These could effectively increase the  
243 concentration of ferrocene carboxylic acid at the surface and thus enhance the current  
244 flow.

245

246 Evidence for this type of behaviour comes from earlier work on DNA where the charge  
247 on the mediator is found to determine the electrochemical response at the surface. DNA is  
248 an anionic polymer due to the presence of phosphate groups and when an anionic  
249 mediator is utilised (ferricyanide), increasing the amount of DNA at the surface by  
250 hybridisation led to a decrease in current transfer due to repulsion and inhibition of

251 mediator diffusion [33]. However when a cationic hexaamine ruthenium mediator was  
252 used, increasing the amount of DNA led to an increase in current transfer [30]. This is  
253 thought to be due to the cationic mediator being bound by the anionic DNA, thereby  
254 increasing the local concentration of mediator at the surface and enhancing electron  
255 transfer between the surface and the probe tip. In a similar fashion we believe the binding  
256 of antigen causes a localised increase of mediator (in this case ferrocene carboxylic acid)  
257 by the same principle and leads to increased current transfer.

258

259 The results demonstrate that NSE is bound at the surface in greater concentration in the  
260 modified areas, indicating that specific binding is indeed occurring. There appears to be  
261 some non-specific binding as shown by the increase in current over the unmodified  
262 carbon surface however, this non-specific binding was only observed at the highest  
263 concentration of  $200 \text{ pg mL}^{-1}$  and not when investigating the lower antigen  
264 concentrations. This confirms our earlier results obtained with microelectrode arrays.<sup>9</sup>  
265 Further confirmation was obtained by control experiments with PSA which showed a low  
266 level of non-specific binding over the entire surface but no specific binding to the anti-  
267 NSE; this is demonstrated in figure 5a.

268

269 In each investigation, an array of twelve dots was imaged with a surface profile being  
270 obtained for each separate dot. The twelve profiles could be combined to give a mean  
271 peak magnitude response for these dots. Figure 5a shows the mean traces for 12 dotted  
272 samples, exposed to a variety of concentrations ( $0.5\text{-}200 \text{ pg ml}^{-1}$ ) of NSE and it is clear  
273 that an increase in tip current as the concentration of antigen increases occurs over the

274 modified regions. For  $200 \text{ pg mL}^{-1}$  the dot profile appears larger and this is believed to be  
275 due to saturation of the area resulting in a much greater level of non-specific binding to  
276 the carbon being observed. There is also sign of the dot swelling in size at 20 and 50  $\text{pg mL}^{-1}$   
277 antigen concentration however, at the lower concentrations ( $0.5\text{-}5 \text{ pg mL}^{-1}$ ) there  
278 is clearly very little change in current to the carbon region. Figure 5b shows a calibration  
279 profile obtained by plotting the peak mean dot responses with respect to antigen  
280 concentration. A linear relationship can be seen between the response and the log of the  
281 concentration in the range  $0.5 \text{ pg mL}^{-1}$  to  $200 \text{ pg mL}^{-1}$ . A logarithmic relationship has  
282 also been found between ac impedance and antigen concentration in previous  
283 immunosensor work [8,10]. This demonstrates the potential for this technique to detect  
284 and quantify the presence of a target in solution.

285

286 The limits of detection for NSE in this experiment ( $0.5 \text{ pg mL}^{-1}$  to  $200 \text{ pg mL}^{-1}$ ) are  
287 comparable to those obtained with sonochemically microfabricated arrays ( $0.5 \text{ pg mL}^{-1}$ )  
288 [12] - and substantially lower than we obtained for similar systems based on  
289 macroelectrodes [7,8,10]. Previous work has succeeded in imaging layers of immobilised  
290 antibodies [34], however their technique required the use of enzyme modified antigens  
291 and also only reported the use of excess labelled antigen whereas our technique is label-  
292 free and is capable of producing a calibration curve. The sensitivity of our method also  
293 compares well with fluorescence based assays, for example when microarrays on silicon  
294 were utilised, antibody-peptide specific interactions could be observed with a detection  
295 limit of  $0.5\text{-}1 \text{ ng mL}^{-1}$  [35, 36].

296

297 The key significance of this work is that for the first time we have demonstrated the  
298 feasibility of SECM antibody based arrays for the development of high throughput  
299 labelless affinity based analysis. This highly simplified approach could in some contexts  
300 directly challenge the fluorescence based approach for molecular diagnostic and/or other  
301 applications.

302

#### 303 **4. Conclusions**

304

305 We have within this paper demonstrated the potential for utilising the SECM to image  
306 arrays of immobilised antibodies and furthermore detect binding of the antigen using a  
307 label-free protocol. A clear relationship between the antigen concentration and the  
308 changes in the signals obtained for binding to the arrays is observed. A calibration profile  
309 showed a clear correlation of change in current with respect to antigen concentration with  
310 detection limits of  $0.5 \text{ pg mL}^{-1}$  to  $200 \text{ pg mL}^{-1}$ . The low ( $\text{pg mL}^{-1}$ ) limits of detection will  
311 aid in the analysis of physiological samples since they can be diluted before use therefore  
312 diminishing the effects of interferents.

313

314 The results obtained within this work demonstrate the feasibility of using the SECM to  
315 analyse surface binding of antigens. This technique although slower than fluorescent  
316 methods, has a significantly lower cost base and does not require labelling of any kind,  
317 including fluorescence of samples. Further work to be conducted will include the  
318 improvement of the preparation of arrays to increase the number of samples being tested  
319 at one time and also to allow for 'control dots' being incorporated within an array.

320

321

322 **Acknowledgements**

323

324 The authors would like to thank Dr Michael Cauchi and Dr Lee Larcombe for help  
325 imaging and formatting scan surfaces as well as Cranfield Health for funding a PhD  
326 project for JLH.

327

328 **References**

329

330 [1] John, R.; Spencer, M.; Wallace, G. G.; Smyth, M. R. *Anal. Chim. Acta.* **1991**, *249*,  
331 381-385.

332

333 [2] Cosnier, S. *Electroanalysis* **2005**, *17*, 1701-1715.

334

335 [3] Diaz-Gonzalez, M.; Gonzalez-Garcia, M. B.; Costa-Garci, A. *Electroanalysis* **2005**,  
336 *17*, 1901-1918.

337

338 [4] Rodriguez-Mozaz, S., de Alda, M. J. L., Barcelo, D. *Anal. Bioanal. Chem.* **2006**,  
339 386, 1025-1041.

340

341 [5] Grant, S.; Davis, F.; Pritchard, J. A.; Law, K. A.; Higson, S. P. J.; Gibson, T. D.  
342 *Anal. Chim. Acta.* **2003**, *495*, 21-32.

343



- 344 [6] Grant, S.; Davis, F.; Law, K. A.; Barton, A. C.; Collyer, S. D.; Higson, S. P. J.;  
345 Gibson, T. D. *Anal. Chim. Acta.* **2005**, *537*, 163-168.  
346
- 347 [7] Garifallou, G-Z.; Tsekenis, G.; Davis, F.; Millner P.A.; Pinacho, D. G.; Sanchez-  
348 Baeza, F.; Marco, M-P.; Gibson, T. D.; Higson, S. P. J. *Anal. Lett.* **2007**, *40*, 1412-  
349 1442.  
350
- 351 [8] Tsekenis, G.; Garifallou, G-Z.; Davis, F.; Millner, P. A.; Pinacho, D. G.; Sanchez-  
352 Baeza, F.; Pilar Marco, M.; Gibson, T. D.; Higson, S. P. J. *Anal. Chem.* **2008**, *80*,  
353 9233-9239.  
354
- 355 [9] Barton, A. C.; Collyer, S. D.; Davis, F.; Garifallou, G.; Tsekenis, G.; Tully, E.;  
356 O’Kennedy, R.; Gibson, T. D.; Millner, P. A.; Higson, S. P. J., *Biosens. Bioelec.*  
357 **2009**, *24*, 1090-1095.  
358
- 359 [10] Tsekenis, G.; Garifallou, G-Z.; Davis, F.; Millner, P. A.; Gibson, T. D.; Higson, S.  
360 P. J. *Anal. Chem.* **2008**, *80*, 2058-2062.  
361
- 362 [11] Barton, A. C.; Davis, F.; Higson, S. P. J. *Anal. Chem.* **2008**, *80*, 6198-6205.  
363
- 364 [12] Barton, A. C.; Davis, F.; Higson, S. P. J. *Anal. Chem.* **2008**, *80*, 9411-9416.  
365
- 366 [13] Barton, A. C.; Davis, F., Higson, S. P. J. *Anal. Lett.* **2010**, in press.

367

368 [14] Wilchek, M.; Bayer, E. A. *Anal. Biochem.* **1988**, *171*, 1-32.

369

370 [15] Pantano, P.; Morton, T. H.; Kuhr, W. G. *J. Am. Chem. Soc.* **1991**, *113*, 1832-1833.

371

372 [16] Martens, P.; Raabe, A.; Johnsson, P. *Stroke* **1998**, *29*, 2363-2366.

373

374 [17] Laskowitz, D.T., Grocott, H., Hsia, A., Copeland, K.R., J. *Stroke Cerebrovascular*  
375 *Diseases* **1998**, *7*, 234-241.

376

377 [18] Missler, U.; Wiesmann, M.; Friedrich, C.; Kaps, M. *Stroke* **1997**, *28*, 1956-1960.

378

379 [19] Yasukawa, T.; Kaya, T.; Matsue, T. *Anal. Chem.* **1999**, *71*, 4637-4641.

380

381 [20] Feng, W.; Rotenberg, S. A.; Mirkin, M. V. *Anal. Chem.* **2003**, *75*, 4148-4154.

382

383 [21] Torisawa, Y., Kaya, T., Takii, Y., Oyamatsu, D., Nishizawa, M., Matsue, T. *Anal.*  
384 *Chem.* **2003**, *75*, 2154-2158.

385

386 [22] Kurulugama, R. T.; Wipf, D. O.; Takacs, S. A.; Pongmayteegul, S.; Garris, P. A.;  
387 Baur, J. E. *Anal. Chem.* **2005**, *77*, 1111-1117.

388

- 389 [23] Torisawa, Y.; Ohara, N.; Nagamine, K.; Kasai, S.; Yasukawa, T.; Shiku, H.; Matsue  
390 T. *Anal. Chem.* **2006**, *78*, 7625-7631.  
391
- 392 [24] Wilherm, T.; Wittstock, G. *Langmuir* **2002**, *18*, 9485-9493.  
393
- 394 [25] Oyamatsu, D.; Hirano, Y.; Kanaya, N.; Mase, Y.; Nishizawa, M.; Matsue, T.  
395 *Bioelectrochemistry* **2003**, *60*, 115-121.  
396
- 397 [26] Suzuki, M.; Yasukawa, T.; Mase, Y.; Oyamatsu, D.; Shiku, H.; Matsue, T.  
398 *Langmuir* **2004**, *20*, 11005-11011.  
399
- 400 [27] Yamada, H.; Fukumoto, H.; Yokoyama, T.; Koike, T. *Anal. Chem.* **2005**, *77*, 1785-  
401 1790.  
402
- 403 [28] Liu, B.; Bard, A. J.; Li, C.; Kraatz, H. *J. Phys. Chem.* **2005**, *109*, 5193-5198.  
404
- 405 [29] Fortin, E.; Mailley, P.; Lacroix, L.; Szunerits, S. *Analyst*, **2006**, *131*, 186-193.  
406
- 407 [30] Roberts, W. S.; Davis, F.; Higson, S. P. J. *Analyst* **2009**, *134*, 1302-1308.  
408
- 409 [31] Schönhoff, M. *Curr. Opin Coll. Inter. Sci.* **2003**, *8*, 86-95.  
410

411 [32] Chai, G.; Brewer, J.M.; Lovelace, L.L.; Aoki, T.; Minor, W.; Lebioda, L. *J. Mol.*  
412 *Biol.* **2004**, *341*, 1015-21.

413

414 [33] Turcu, F.; Schulte, A.; Hartwich, G.; Schuhmann, W. *Biosens. Bioelec.* **2004**, *20*,  
415 925–932.

416

417 [34] Wittstock, G.; Yu, K-J.; Halsall, H. B.; Ridgway, T. H.; Heineman, W. R. *Anal.*  
418 *Chem.* **1995**, *67*, 3578-3582.

419

420 [35] Cretich, M.; Damin, F.; Longhi, R.; Gotti, C.; Galati, C; Renna, L.; Chiari, M.  
421 *Methods Mol. Biol.* **2010**, *669*, 147-160.

422

423 [36] Cretich, M.; di Carlo, G.; Longhi, R.; Gotti, C.; Spinella, N.; Coffa, S.; Galati, C.;  
424 Renna, L.; Chiari, M. *Anal. Chem.* **2009**, *81*, 5197–5203.

425

## 426 **Figure Captions**

427

428 Figure 1. (a) Schematic representation of SECM instrumentation- the microelectrode  
429 probe is clamped into a high resolution XYZ micropositioning device and scanned across  
430 the sample surface. Scan parameters and tip electrochemistry are controlled via a PC  
431 interface. (b) The arrangement of electrodes in the electrochemical cell – i.e. WE, RE and  
432 the CE. (c) Redox coupling of ferrocene carboxylic acid between the microelectrode tip  
433 and the substrate.

434

435 Figure 2. Photograph of biotinylated PEI deposition on carbon electrode by pulled  
436 microcapillary using the XYZ micro-positioning stage of the SECM270 and of the final  
437 array pattern on the screen printed carbon electrode surface (dot size ~ 200  $\mu\text{m}$ ).

438

439 Figure 3. Area scan of PEI/avidin/biotinylated antibody arrays on screen printed carbon  
440 electrode (a) before and (b) following rinsing and 30 mins exposure to water; (c) absolute  
441 change in measured current. (Scan rate was 10  $\mu\text{m}$  per step). (Note Z axis scales are in  
442 reverse for visual aid).

443

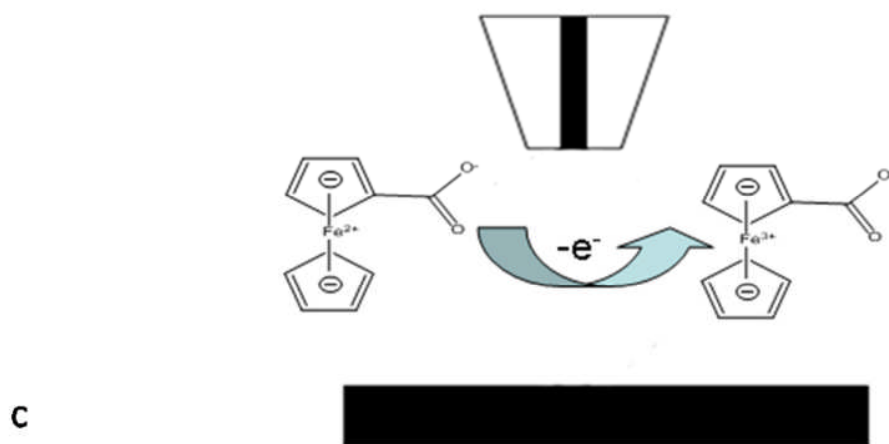
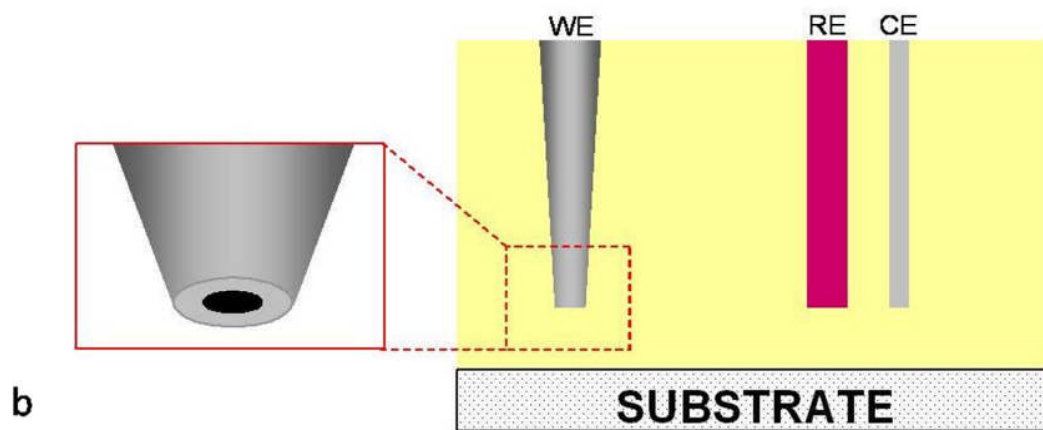
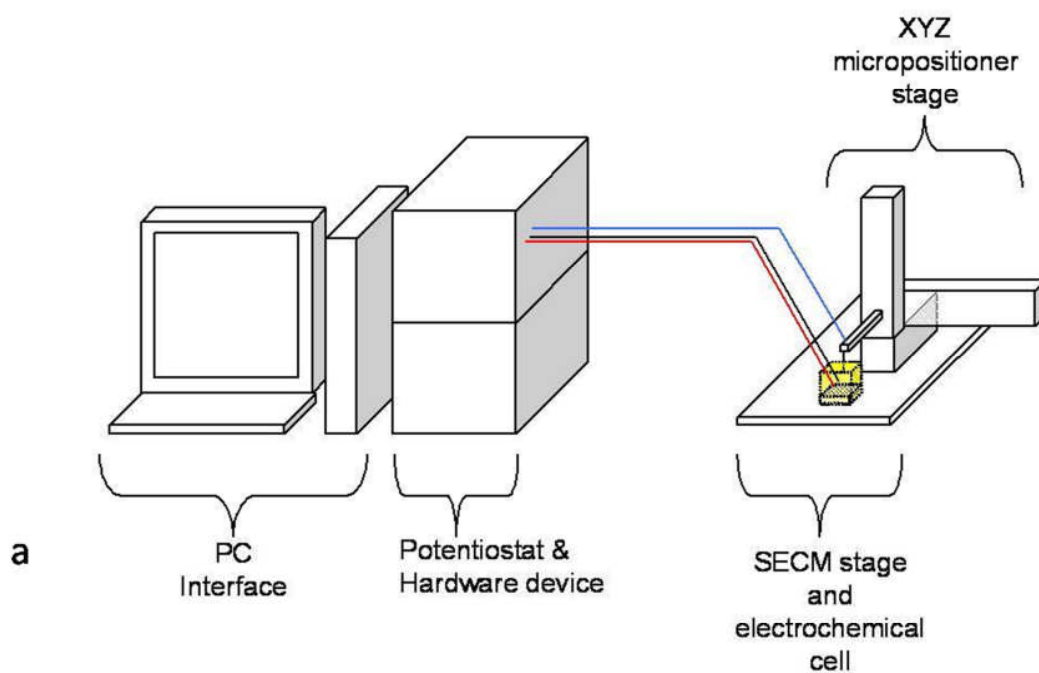
444 Figure 4. SECM scan of a PEI/avidin/biotinylated antibody array on a screen-printed  
445 carbon electrode; (a) following exposure to biotinylated antibody NSE, (b) following  
446 further exposure to complementary NSE antigen at 200  $\text{pg mL}^{-1}$ , (c) absolute change in  
447 measured current. (Scan rate was 10  $\mu\text{m}$  per step). (Note Z axis scales are in reverse for  
448 visual aid).

449

450 Figure 5. (a) Mean changes of a twelve dot array scan ( $n = 12$ ) taken over  
451 PEI/avidin/biotinylated antibody surface area to various antigen concentrations (no error  
452 bars are included for clarity, data points on individual curves represent the tip current  
453 values taken in different sites of the dots); (b) Calibration plot showing changes in current  
454 measured ( $n = 12$ ) vs. NSE concentration. Equation is  $y = 0.54\ln(x) + 0.51$ ,  $R^2=0.97$  and  
455 the error bars show the standard deviation between the 12 individual dots.

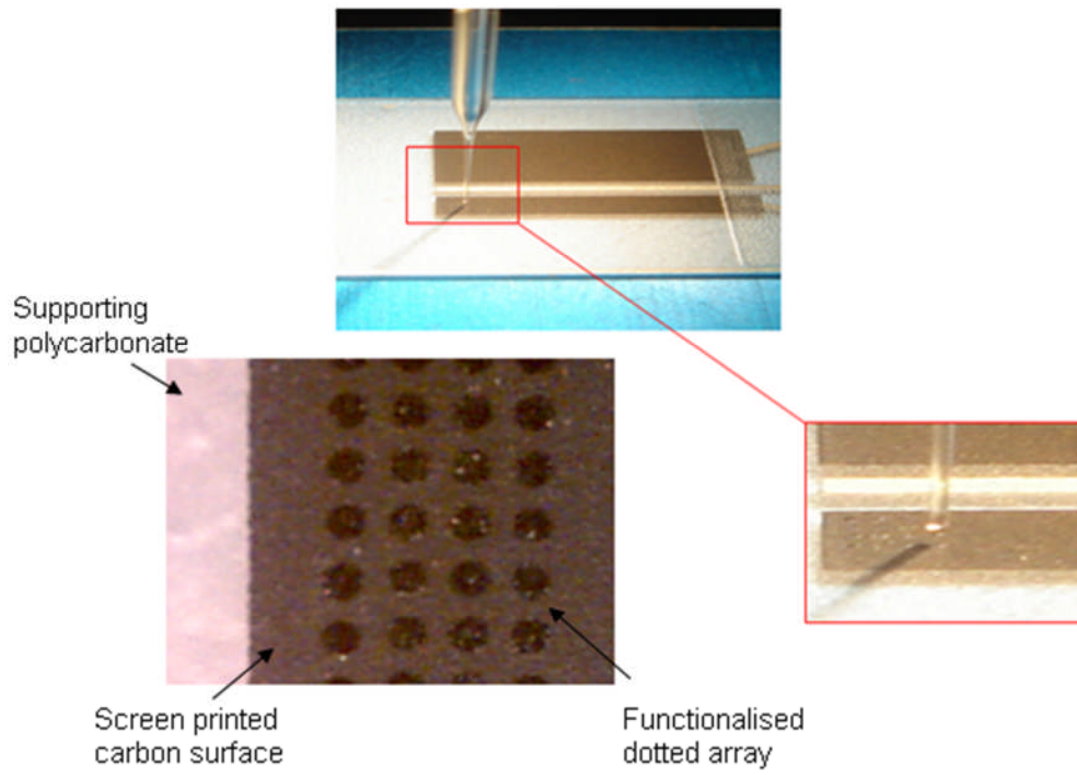
456

457 Figure 1.



458

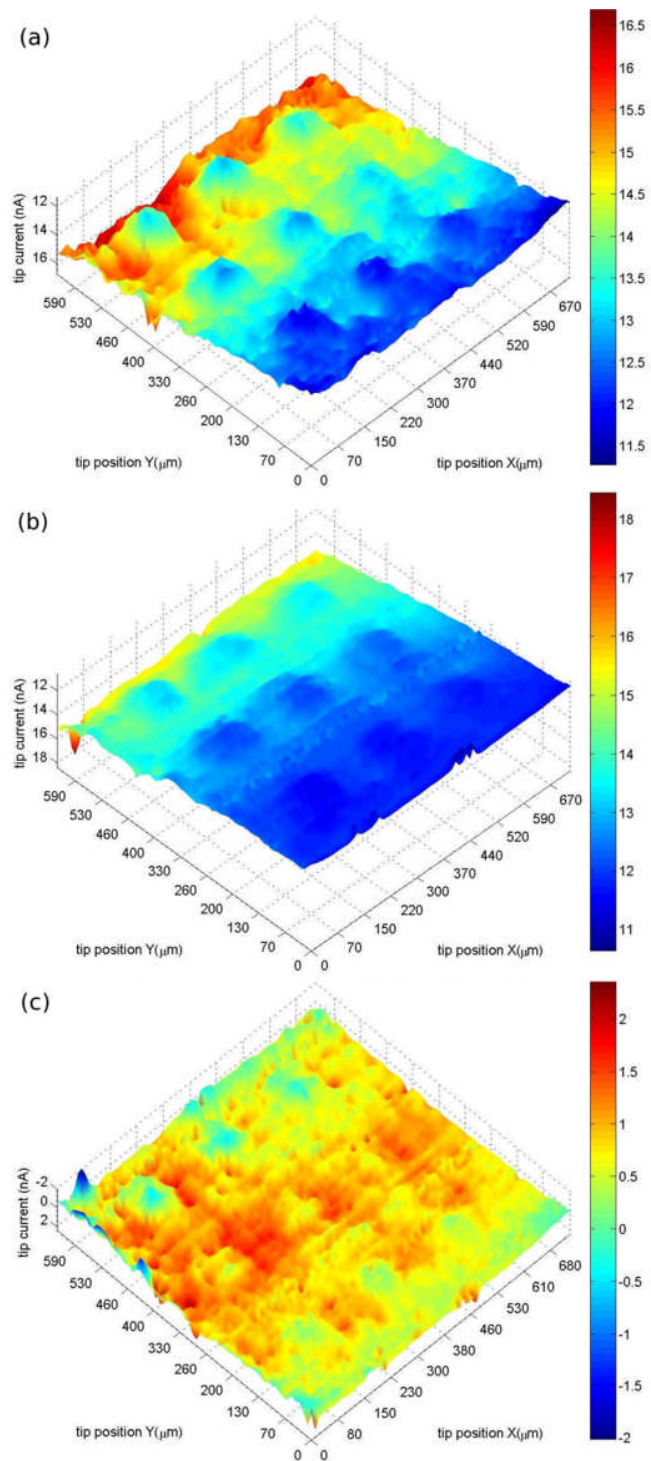
459 Figure 2.



460

461

462 Figure 3.

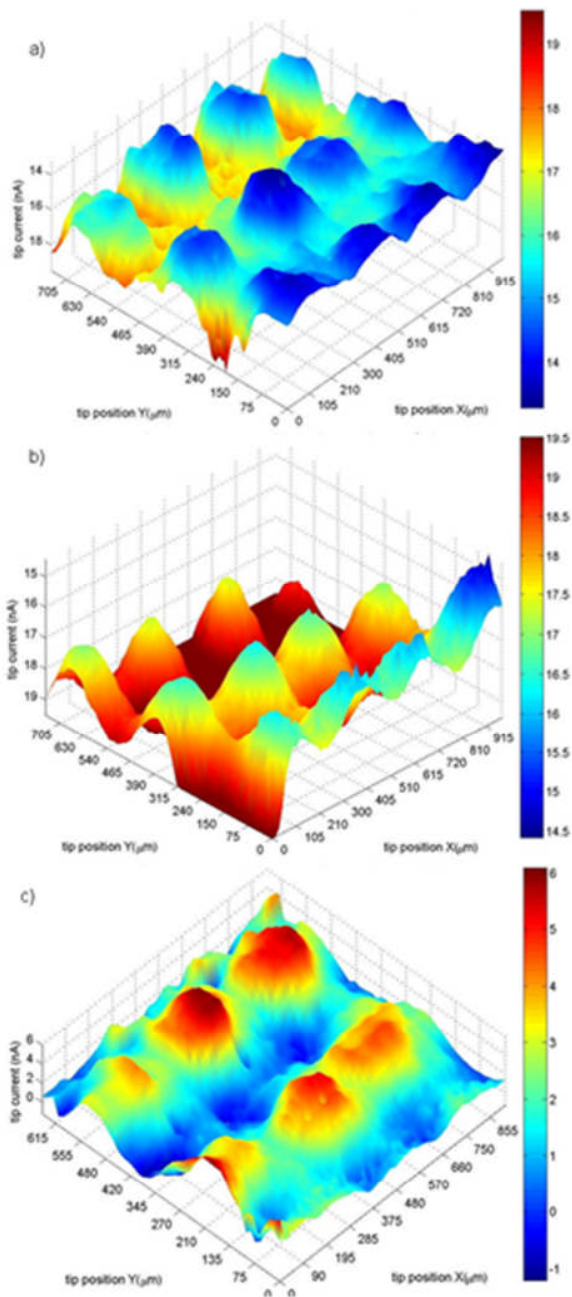


463

464



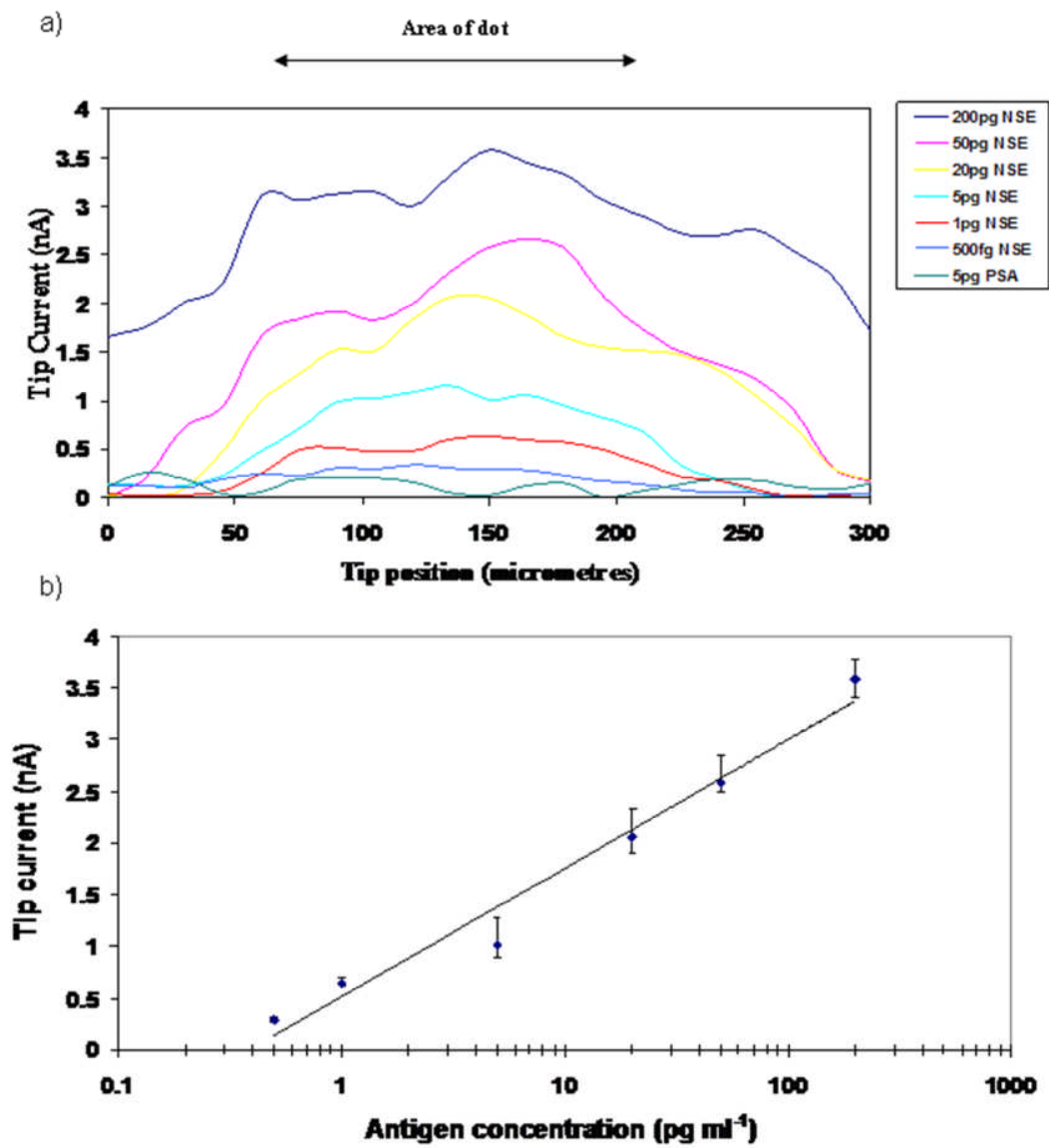
465 Figure 4.



466

467

468 Figure 5.



469